



1 Overcoming model instability in tree-ring-based temperature 2 reconstructions using a multi-species method: A case study from the 3 Changbai Mountains, northeastern China

4 Liangjun Zhu^{1,2}, Shuguang Liu¹, Haifeng Zhu³, David J. Cooper⁴, Danyang Yuan², Yu Zhu¹, Zongshan Li⁵,
5 Yuandong Zhang⁶, Hanxue Liang⁷, Xu Zhang⁸, Wenqi Song², Xiaochun Wang^{2,*}

6 ¹National Engineering Laboratory for Applied Technology of Forestry & Ecology in South China, College of Life Science and Technology,
7 Central South University of Forestry and Technology, Changsha 410004, China

8 ²Center for Ecological Research and Key Laboratory of Sustainable Forest Ecosystem Management-Ministry of Education, School of
9 Forestry, Northeast Forestry University, Harbin 150040, China

10 ³Institute of Tibetan Plateau Research, Chinese Academy of Sciences, Beijing 100864, China

11 ⁴Department of Forest and Rangeland Stewardship, Colorado State University, Fort Collins, CO 80523, USA

12 ⁵State Key Laboratory of Urban and Regional Ecology, Research Center for Eco-Environmental Sciences, Chinese Academy of Sciences,
13 Beijing 100085, China

14 ⁶Key Laboratory of Forest Ecology and Environment of National Forestry and Grassland Administration, Research Institute of Forest
15 Ecology, Environment and Protection, Chinese Academy of Forestry, Beijing 100091, China

16 ⁷Institute of Loess Plateau, Shanxi University, Taiyuan 030006, China

17 ⁸College of Forestry, Northwest A&F University, Yangling 712100, China

18 *Correspondence to: Xiaochun Wang (wangx@nefu.edu.cn)

19 **Abstract.** The unstable sensitivity of growth-climate relationships greatly restricts tree-ring-based paleoclimate reconstructions,
20 especially in areas with frequent “divergence” problems, such as the temperate zone in northeast China. Here, we propose an original
21 tree-species mixing method to overcome this obstacle and improve the stability and reliability of reconstruction models. We take the
22 tree-ring based growing-season minimum temperature reconstruction for the northern Changbai Mountains in northeast China as an
23 example to illustrate the method. Compared with previous temperature reconstruction models, our reconstruction model is more
24 stable and reliable and explains up to 68% of the variance. It is also highly consistent with historical records and tree-ring-based
25 temperature reconstructions from the nearby Xiaoxing’an Mountains and from across the Northern Hemisphere. Our reconstruction
26 uses two different tree species and is more accurate than temperature reconstructions developed from a single species. Over the past
27 259 years (AD 1757-2015), five significant cold periods and five warm periods were identified. The reconstruction indicates rapid
28 warming since the 1980s, which is consistent with other instrumental and reconstructed records. We also found the Atlantic
29 Multidecadal Oscillation plays a crucial role in driving the growing-season minimum temperature in the northern Changbai
30 Mountains.

31 1 Introduction

32 Global climates are changing rapidly, with unexpected consequences; in fact, climate change is a major threat to ecosystems and
33 societies in many parts of the world (IPCC, 2018; Allen et al., 2010; Liu et al., 2013). Understanding and quantifying the
34 characteristics, patterns, and driving mechanisms of past climate changes is essential to reducing the uncertainty in predicting future



35 climates (Fritts, 1976;Zhu et al., 2020a). However, the lack of long-term instrumental climate data severely limits our ability to
36 understand past climates; for this reason, long climate proxy records are urgently needed.

37 Tree rings, especially ring widths, are a critically important paleoclimate proxy (Fritts, 1976) and are widely used for reconstructing
38 climate at a high resolution over hundreds to thousands of years (Anchukaitis et al., 2017;Wilson et al., 2016). Such records are
39 invaluable for placing recent climatic changes in a long-term context, which can help considerably with planning appropriate
40 responses to future climate changes and extreme events. However, the statistical calibration and verification of tree-ring based
41 reconstructions is a rigorous process (Fritts, 1976) that requires a relatively stable growth-climate relationship over time.

42 Over the last several decades, many studies have addressed the “divergence problem”, an anomalous reduction in tree-ring indices
43 and temperature sensitivity after rapid warming (D'Arrigo et al., 2008). Other studies have found an increased correlation between
44 tree-ring indices and temperature after rapid warming, such as in the case of *Fraxinus mandshurica* (FM) (Cao et al., 2018) and *Larix*
45 *gmelinii* (Zhang et al., 2016) in northeastern China. These two types of “unstable sensitivity” in growth-climate relationships
46 challenge the assumption of “uniformity principle” in dendroclimatology (Fritts, 1976), and thus brings more uncertainties in tree-
47 ring-based inferences on past climate.

48 The Changbai Mountains are the highest in eastern Eurasia, covering nearly 2,000 square kilometers. Climate changes in the region
49 significantly affect human social-economic activities and ecosystem health. A number of tree-ring-based reconstructions have been
50 carried out in the region in the past two decades (Zhu et al., 2009;Shao and Wu, 1997;Lyu et al., 2016;Zhang et al., 2007;Wang et al.,
51 2012;Yu, 2019). These studies have looked at the tree-ring widths of *Pinus koraiensis* (Zhu et al., 2009;Shao and Wu, 1997;Lyu et
52 al., 2016) and *F. mandshurica* (Zhang et al., 2007;Wang et al., 2012;Yu, 2019). However, some other studies report an evident
53 unstable sensitivity in the growth-climate relationships of *Pinus koraiensis* and *F. mandshurica*'s both before and after warming (Cao
54 et al., 2018;Zhu et al., 2020b). These two species typify the two types of unstable growth-climate (temperature) relationships (*P.*
55 *koraiensis*: reduced sensitivity and *F. mandshurica*: increased sensitivity) in temperate forests, northeastern China (Cao et al.,
56 2018;Zhu et al., 2015b;Zhu et al., 2020b;Wang et al., 2016). For this reason, climate reconstructions that are based on only one
57 species' tree-ring data may be biased toward that species' specific response to climate (Lyu et al., 2016;Wang et al., 2012).

58 In this study, we propose a hypothesize that the accuracy of reconstruction in areas with frequent “unstable sensitivity” problems can
59 be improved through mixing two species typifying the two types of unstable growth-climate (temperature) relationships. The
60 Changbai Mountains are especially prone to the unstable sensitivity in growth-climate relationships due to rapid warming (Cao et al.,
61 2018;Zhu et al., 2020b;Zhu et al., 2018a). Hence, we use trees from the Changbai Mountains as an example by compositing tree-ring



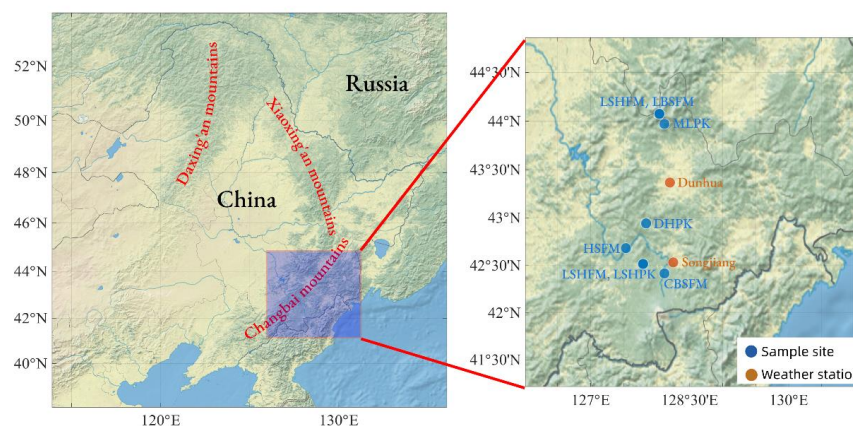
62 data from species experiencing different types of unstable sensitivity. We aim to (1) develop a new tree-ring-based temperature
63 reconstruction for the Changbai Mountains by a mixing multi-species method; (2) verify and compare its accuracy and consistency
64 with other temperature records; (3) identify the patterns of past temperature changes and possible large-scale driving mechanisms.

65 2 Materials and methods

66 2.1 Study area

67 The study area is located in the northern part of the Changbai Mountains (Fig. 1). It is characterized by a temperate continental
68 monsoon climate with four distinct seasons. Based on climate data (<http://data.cma.cn/>) from the Songjiang and Dunhua
69 meteorological stations, the average annual temperature in the study area ranges from 1.3 °C to 4.85 °C. January (-17.08 °C) and July
70 (20.13 °C) are the coldest and warmest months, respectively (Fig. 2). The mean annual total precipitation is 652 mm (335-734 mm),
71 and 87.05% of the annual precipitation falls during the growing season (April to September) (Fig. 2). Over the past 60 years, the
72 average minimum temperature has increased significantly ($p < 0.01$) at a rate of 0.06 °C per year. There has been no significant
73 change in the total annual precipitation (Fig. 2a-c).

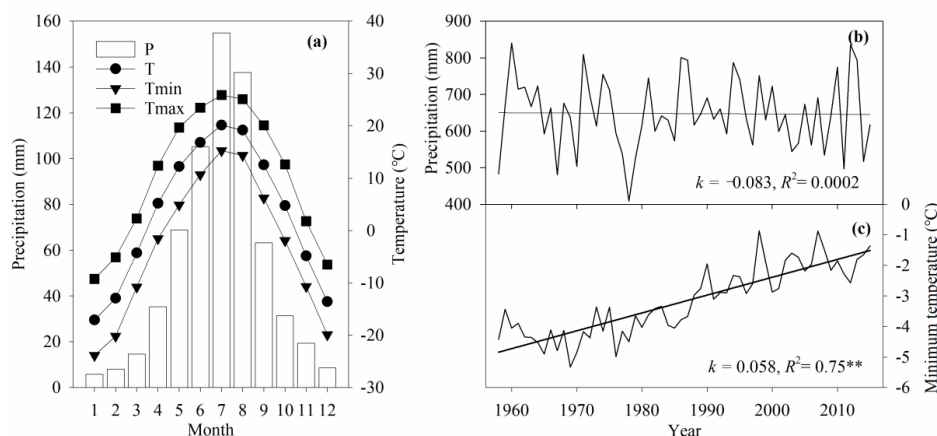
74 We carried out our study in the lower and middle elevation areas (700-1100 m a.s.l.) of the northern Changbai Mountains. All
75 sampling sites are characterized by typical broadleaf-Korean pine mixed forests with little human disturbance. Such forests represent
76 the zonal climax vegetation type of the temperate regions in northeastern China. The main tree species include *P. koraiensis*, *Abies*
77 *nephrolepis*, *Picea jezoensis* var. *microsperma*, *F. mandshurica*, *Phellodendron amurense*, *Juglans mandshurica*, *Tilia amurensis*,
78 *Betula costata*, *Quercus mongolica*, and *Ulmus japonica*. The soils are mainly dark-brown forest soil.



79
80 **Figure 1.** Map showing the distribution of sampling sites and weather stations in the study. This figure was drawn by MATLAB R2017b
81 software (The MathWorks, Inc.). The basemap, presented with a light, natural palette, overlaid with the boundary line, combines satellite-



82 derived land cover data, shaded relief, and ocean-bottom relief made with Natural Earth. MathWorks® offers the basemap with
83 geographic axes and charts.



84
85 **Figure 2. Monthly distribution and inter-annual variability of climate variables in the northern Changbai Mountains. (a) Mean (T),**
86 **minimum (T_{min}), and maximum (T_{max}) temperature and the monthly distribution of total precipitation (P). The inter-annual variability of**
87 **(b) total precipitation and (c) minimum temperature. The climate data for the period 1958-2016 were averaged using records from the**
88 **Songjiang (42.533°N, 128.25° E, 525 m a.s.l.) and Dunhua (43.367°N, 128.2° E, 591 m a.s.l.) meteorological stations.**

89 2.2 Tree-ring data

90 From May to August in 2012, 2014, and 2016, at least one core per tree was extracted at breast height (1.3 m) from both *P. koraiensis*
91 and *F. mandshurica* trees at six forest sites in the Changbai Mountain using 5.15-mm increment borers. A total of 433 cores from 259
92 trees were used in this study (Table S1).

93 All tree-ring cores were mounted, dried, and progressively surfaced in the laboratory until individual cells within annual rings were
94 visible under a dissecting microscope. The cores were then visually cross-dated using the skeleton plot method to identify absent or
95 false rings (Fritts, 1976; Stokes and Smiley, 1968). Ring widths were measured to a precision of 0.001 mm using the Velmex Tree-ring
96 Measurement System (Velmex, Bloomfield, NY, USA). The COFECHA program was used to check the quality of cross-dating and
97 measurement (Holmes, 1983). Conservative negative exponential curves or linear regression curves of any slope were used to remove
98 age-related growth trends. Tree-ring chronologies were developed using the R package 'dplR' (Bunn, 2008). The inter-series correlation
99 (R_{bar}) and expressed population signal (EPS) were used to control the quality of the chronologies (Table S1) (Wigley et al., 1984).

100 2.3 Climate data and other records

101 Instrumental climate data, including monthly total precipitation and mean, minimum, and maximum temperature, were obtained for



102 the Songjiang and Dunhua meteorological stations from the China Meteorological Data Service Center (<http://data.cma.cn/>). The
103 distance between the eight sampling sites and its nearest weather station is between 20 and 80 km. The regional climate during the
104 growing season (April to September) was calculated by taking the arithmetic average of the data from the two weather stations (Fig.
105 2).

106 The actual (Enfield et al., 2001) and reconstructed (Mann et al., 2009; Gray, 2004) Atlantic Multidecadal Oscillation (AMO) index
107 was downloaded from <http://climexp.knmi.nl/> and <https://www.ncdc.noaa.gov/paleo-search/study/6324>. All reference tree-ring-based
108 temperature sequences used in this study were requested from the authors of the relevant studies.

109 **2.4 Statistical analyses and model verification**

110 Pearson correlation and moving correlation methods were used to check the relationships between the chronologies. Correlation
111 analysis was used to identify the relationship between the tree-ring chronology and regional monthly or seasonal climate records. A
112 simple linear regression model was used to reconstruct the growing-season minimum temperature for the northern Changbai
113 Mountains. A traditional split-period calibration-verification method was used to test the regression model's goodness-of-fit (stability
114 and reliability) (Fritts, 1976).

115 Statistical parameters including the correlation coefficient (R), explained variance (R^2), reduction of error (RE), coefficient of
116 efficiency (CE) and sign test (ST) were used to verify the model. RE indicates whether a reconstruction provides a better estimate of
117 climate variability than simply using the mean value of the target climate in the calibration period. CE is similar to RE, but it tests
118 reconstruction skill against the mean value of the target climate in the verification period. RE and CE are rigorous verification
119 statistics; any positive RE and CE values indicate sufficient similarity between the estimated and actual sequences. Thus, positive RE
120 and CE values indicate that the model has a considerable predictive skill (Fritts, 1976). The ST was used to test the coherency
121 between the actual and estimated series by calculating the coherence and incoherence (Fritts, 1976).

122 To explore our reconstruction's spatial representativeness, we performed a spatial correlation between the actual and estimated
123 growing-season minimum temperature and the April-September gridded ($0.5^\circ \times 0.5^\circ$) CRU TS4.04 minimum temperature for the
124 period 1958-2015 using the KNMI Climate Explorer (<http://climexp.knmi.nl/>). We defined warm (cold) periods as periods of at least
125 two consecutive years during which the 10-year low-pass filtered temperature value was greater than (less than) high than the
126 average (a) plus (minus) 0.5 times the standard deviation (δ) (8.3°C for warm periods, 7.7°C for cold periods). We used the multi-
127 taper method of spectral analysis to identify the periodicity of temperature variability (Mann and Lees, 1996). This method is
128 especially suitable for diagnosing and analyzing weak signals and has been widely used to analyze paleoclimate signals (Liu et al.,



129 2019).

130 To better ascertain the accuracy of our temperature reconstruction and its consistency with regional records, we compared it with nearby
131 temperature records and local historical documents. We used direct comparisons of curve trends and Pearson correlations to evaluate
132 the consistency of our growing-season minimum temperature reconstruction and nearby tree-ring based temperature reconstructions.
133 A 10-year low-pass loess filtering method was used to highlight the low-frequency signals of temperature records and the actual
134 (Enfield et al., 2001) and reconstructed Atlantic Multi-decadal Oscillation (AMO) data. Z-scores were used to normalize the
135 temperature records and ensure that they were kept at the same scale. Pearson correlation was used to evaluate the relationship between
136 our temperature reconstruction and the AMO index. To further verify the influence of the AMO on local temperature, we conducted a
137 spatial correlation between our temperature reconstruction and global gridded sea surface temperatures (SST) (HadISST1 SST dataset,
138 $1^{\circ} \times 1^{\circ}$, 1870-2015) using the KNMI Climate Explorer (<http://climexp.knmi.nl>). The 20th century reanalysis data were used to produce
139 composite maps of the 500-mb vector wind and air temperature from April to September. These maps were then used to explore the
140 linkages between temperature and atmospheric circulation patterns in the Northern Hemisphere.

141 **3 Results**

142 **3.1 Consistency of tree growth and its response to climate**

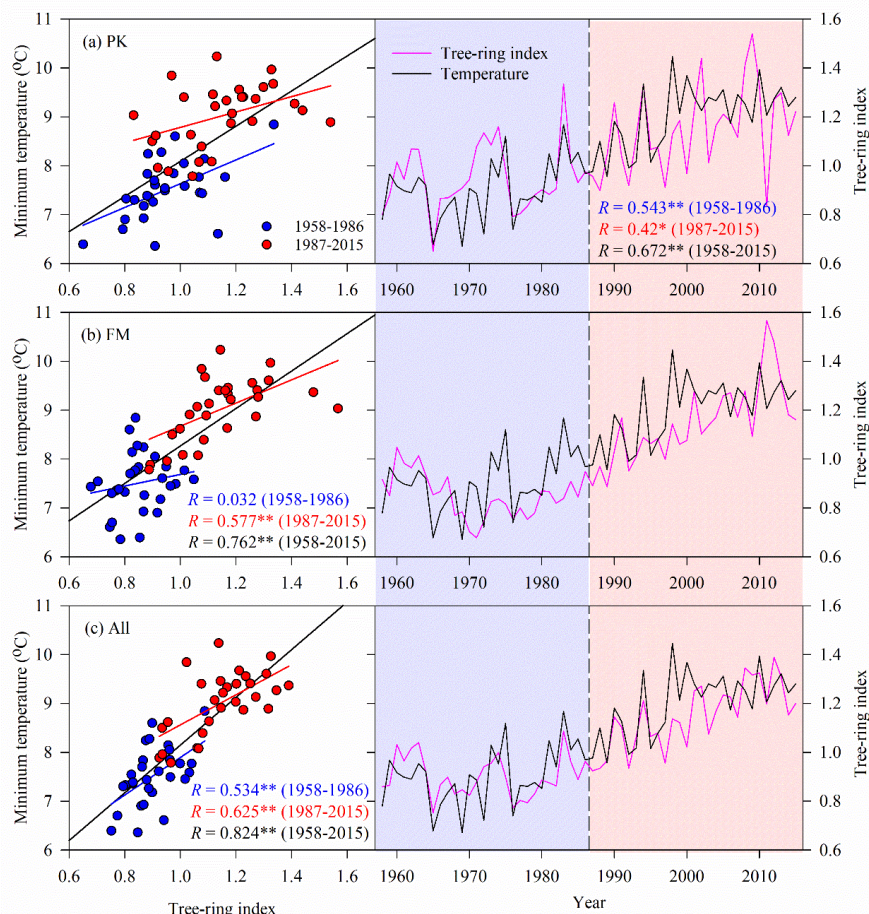
143 For both *P. koraiensis* and *F. mandshurica*, significant correlations exist among all site chronologies over their common period of 1855-
144 2011 (Table S2). Significant correlations between *P. koraiensis* and *F. mandshurica* chronologies, however, only exist for some sites.
145 The mixed-species regional chronology (ALL, in Table S2) correlates significantly with each site chronology and each combined
146 species chronology (Table S2).

147 Growing-season minimum temperature strongly affects the growth of both *P. koraiensis* and *F. mandshurica* in Changbai Mountains.
148 Most sites' tree-ring indices correlate significantly ($p < 0.05$) with April, May, June, July, August, and September minimum
149 temperatures (Table 1). The radial growth of *P. koraiensis* and *F. mandshurica* at all sites is positively correlated with the mean growing-
150 season (April-September) minimum temperature. The three combined chronologies (PK, FM, and ALL in Table 1) are all significantly
151 correlated with growing-season minimum temperature; the highest positive correlation is found between the mixed-species regional
152 chronology (ALL) and the growing-season minimum temperature ($R = 0.824$, $p < 0.001$).

153 However, there is a differential temporal instability in the growth-climate relationship between *P. koraiensis* and *F. mandshurica*. For
154 the combined *P. koraiensis* chronology (PK), there is a stronger positive correlation with the growing-season minimum temperature



155 during the period 1958-1986 than the period 1987-2015. For the combined *F. mandshurica* chronology (FM), the correlation is stronger
 156 during the second period than the first. However, the mixed-species regional chronology (ALL) shows significant correlations in both
 157 the first and second periods (Table 1 & Fig. 3).



158
 159 **Figure 3.** Correlation relationships between the growing-season minimum temperature and the combined *P. koraiensis* (PK), the combined
 160 *F. mandshurica* chronology (FM), and mixed-species regional chronologies (ALL) during the first part of the chronology (1958-1986)
 161 and second part (1987-2015).

162 **Table 1.** Correlations between the site and regional chronologies and regional minimum temperature during the growing season (current
 163 April to current September).

	Apr	May	Jun	Jul	Aug	Sep	Apr-Sep
DHPK ($n = 54$)	0.59^{**}	0.48^{**}	0.22	0.28[*]	0.08	0.51^{**}	0.51^{**}
LBSPK ($n = 58$)	0.58^{**}	0.66^{**}	0.65^{**}	0.53^{**}	0.22	0.54^{**}	0.73^{**}
LSHPK ($n = 57$)	0.34^{**}	0.25	0.19	0.23	0.12	0.40^{**}	0.36^{**}
MLPK ($n = 58$)	0.31[*]	0.41^{**}	0.35^{**}	0.39^{**}	0.37^{**}	0.42^{**}	0.51^{**}
CBSFM ($n = 56$)	0.43^{**}	0.65^{**}	0.63^{**}	0.48^{**}	0.46^{**}	0.54^{**}	0.73^{**}



HSFM ($n = 57$)	0.56**	0.71**	0.72**	0.50**	0.46**	0.57**	0.81**
LBSFM ($n = 58$)	0.37**	0.52**	0.60**	0.53**	0.40**	0.48**	0.66**
LSHFM ($n = 57$)	0.36**	0.55**	0.53**	0.43**	0.41**	0.48**	0.63**
PK ($n = 58$)	0.58**	0.58**	0.46**	0.45**	0.25	0.59**	0.67**
FM ($n = 58$)	0.47**	0.66**	0.67**	0.52**	0.46**	0.55**	0.76**
ALL ($n = 58$)	0.60**	0.71**	0.65**	0.56**	0.41**	0.66**	0.82**

164 Notes: * = $p < 0.05$, ** = $p < 0.01$. Tree-ring indices of combined *P. koraiensis* (PK), combined *F. mandshurica* (FM), and mixed species (ALL) were
 165 calculated using a simple arithmetic average.

166 3.2 Tree-ring-based minimum temperature reconstruction

167 We attempted to reconstruct the growing-season minimum temperature for the northern Changbai Mountains based on the FM, PK,
 168 and ALL chronologies using a linear regression model. Neither the FM nor the PK chronology is suitable for the reconstruction due to
 169 negative CE and insignificant ST tests (Table 2). However, the ALL chronology combined with the FM and PK chronologies passes
 170 the model test. The model equation is the following:

$$171 T_t = 4.881 * I_t + 3.268, (R = 0.824, N = 57, F = 118.74, p < 0.0001) \quad (1)$$

172 where the T_t and I_t are the growing-season minimum temperature and regional tree-ring index at the year t , respectively.

173 Table 2. Calibration and verification statistics for the growing-season mean temperature reconstruction.

	Calibration	R	Verification	R^2	RE	CE	ST
PK	1958-2015	0.67**	—	0.45**	0.45	—	(42, 16)**
	1987-2015	0.42*	1958-1986	0.30**	0.84	-0.22	(20, 9)
	1958-1986	0.54**	1987-2014	0.18*	0.77	-0.50	(20, 9)
FM	1958-2015	0.76**	—	0.58**	0.58	—	(49, 9)**
	1987-2015	0.58**	1958-1986	0.03	0.83	-0.23	(16, 13)
	1958-1986	0.18	1987-2014	0.33**	0.87	0.12	(23, 6)**
ALL	1958-2015	0.82**	—	0.68**	0.67	—	(49, 9)**
	1987-2015	0.63**	1958-1986	0.29**	0.89	0.20	(21, 8)*
	1958-1986	0.53**	1987-2014	0.39**	0.88	0.20	(22, 7)**

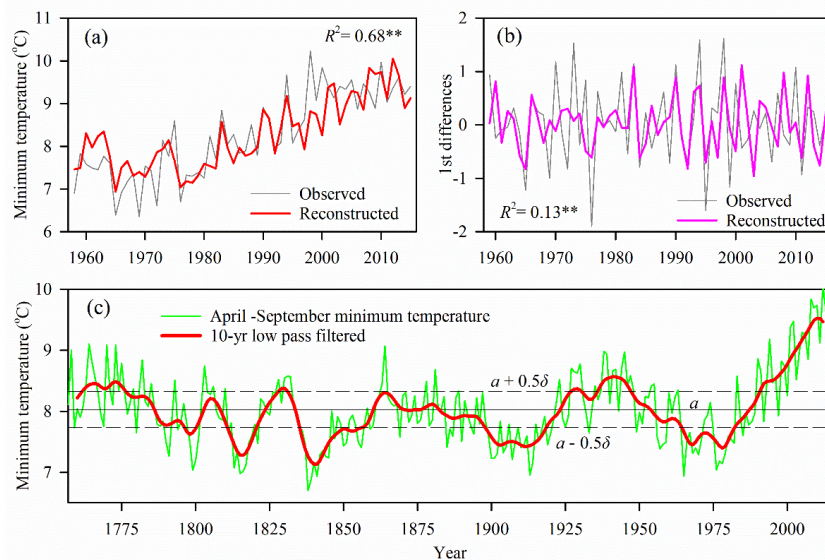
174 Notes: Statistical parameters that are not significant or that failed the verification test are highlighted in bold. * = $p < 0.05$, ** = $p < 0.01$.

175

176 The model explains 68% of the temperature variation. A similar or parallel trend is found between the reconstructed and observed
 177 growing-season minimum temperatures ($R^2 = 0.68, p < 0.01$) and between their first-order differences ($R^2 = 0.13, p < 0.01$) during the
 178 calibration period from 1958 to 2015 (Fig. 4a & 4b). A significant spatial correlation pattern is found between the actual and
 179 reconstructed growing-season minimum temperature and the gridded ($0.5^\circ \times 0.5^\circ$) April-September averaged CRU TS4.04 minimum



180 temperature over northeast Asia (Fig. S3). The positive RE and CE in the verification periods (Table 2) indicate that our reconstruction
181 model has a robust skill and acceptable reliability in estimating the growing-season temperature (Fritts, 1976). The R^2 and ST statistics
182 are all significant at the 95% or 99% confidence levels, which indicates that our model is stable and reliable in the two calibration
183 periods (Table 2).



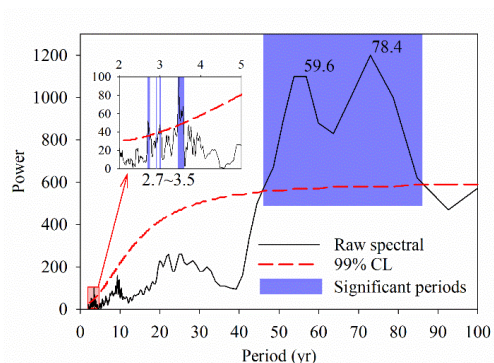
184
185 **Figure 4. Minimum temperature reconstruction for the northern Changbai Mountains, northeastern China. (a) Comparisons between**
186 **reconstructed and observed April-September minimum temperature during the calibration period 1958-2015. (b) Comparisons between**
187 **the first-order differences of reconstructed and observed April-September minimum temperatures for the period 1959-2014. (c) April-**
188 **September minimum temperatures for the northern Changbai Mountains from 1757 to 2015 (cyan line) with a 10-year low-pass filter (red**
189 **line). The α and δ indicate the average (8.03) and standard deviation (0.59) values of the minimum temperature during the whole span,**
190 **respectively.**

191 3.3 Growing season temperature variations

192 In the northern Changbai Mountains, the growing-season minimum temperature has a high interannual and decadal variance with a
193 mean (α) of 8.03 and a standard deviation (δ) of ± 0.59 during the past 259 years (Fig. 4c). The record contains five warm periods
194 (1762-1776, 1828-1831, 1927-1930, 1936-1947, and 1991-2012) and five cold periods (1797-1800, 1811-1820, 1836-1856, 1898-
195 1918, and 1956-1982) (Table 3). The periods 1991-2012 and 1836-1856 are the most prolonged and most severe warm and cold periods,
196 respectively. Most cold years/periods occur during the 19th century, and most warm years/periods occur during the 20th century. There
197 is a clear rapid warming trend after the 1980s. The top ten warmest and coldest years are listed in Table 3. Spectral analysis of the full
198 reconstruction (1757-2015) reveals significant ($p < 0.01$) annual cycle peaks at 2.7, 3, and 3.5 years, and decadal cycle peaks at 59.6



199 and 78.4 years (Fig. 5).



200

201 **Figure 5. Multi-taper power spectra for the growing-season minimum temperatures from AD 1757 to 2015 in the northern Changbai**
 202 **Mountains. The 99% confidence level relative to red noise is shown by the dashed red line. The lengths of the sig nificant cycles are**
 203 **indicated in the figure.**

204 **Table 3. The top 10 most extreme warm/cold years and extreme warm/cold periods in the northern Changbai Mountains.**

Rank	Warm/Cold years				Warm/Cold periods			
	Cold	Tmin	Warm	Tmin	Period	Duration	Mean	Warm/Cold
1	1838	6.71	2012	10.05	1762-1776	15	8.47	Warm
2	1839	6.88	2008	9.83	1797-1800	4	7.38	Cold
3	1841	6.93	2010	9.74	1811-1820	10	7.39	Cold
4	1965	6.94	2009	9.69	1828-1831	4	8.44	Warm
5	1913	6.96	2013	9.66	1836-1856	21	7.46	Cold
6	1815	6.98	2002	9.47	1898-1918	21	7.50	Cold
7	1816	7.01	2001	9.37	1927-1930	4	8.69	Warm
8	1799	7.03	2005	9.30	1936-1947	12	8.55	Warm
9	1976	7.04	2006	9.26	1956-1982	18	7.47	Cold
10	1813	7.07	1994	9.18	1991-2012	22	8.90	Warm

205 4 Discussion

206 4.1 Climate-growth relationships and their stability

207 We found that the radial growth of *P. koraiensis* and *F. mandshurica* is significantly positively correlated with growing-season
 208 minimum temperature. This result is consistent with those of other dendrochronological studies of *P. koraiensis* (Zhu et al., 2009;Shao
 209 and Wu, 1997) and *F. mandshurica* (Zhu et al., 2015a;Li and Wang, 2013;Zhu et al., 2020b) in northeastern China, and of other species
 210 at high latitudes in the Northern Hemisphere (Zhu et al., 2020b;Anchukaitis et al., 2017;Wilson et al., 2016). High growing-season



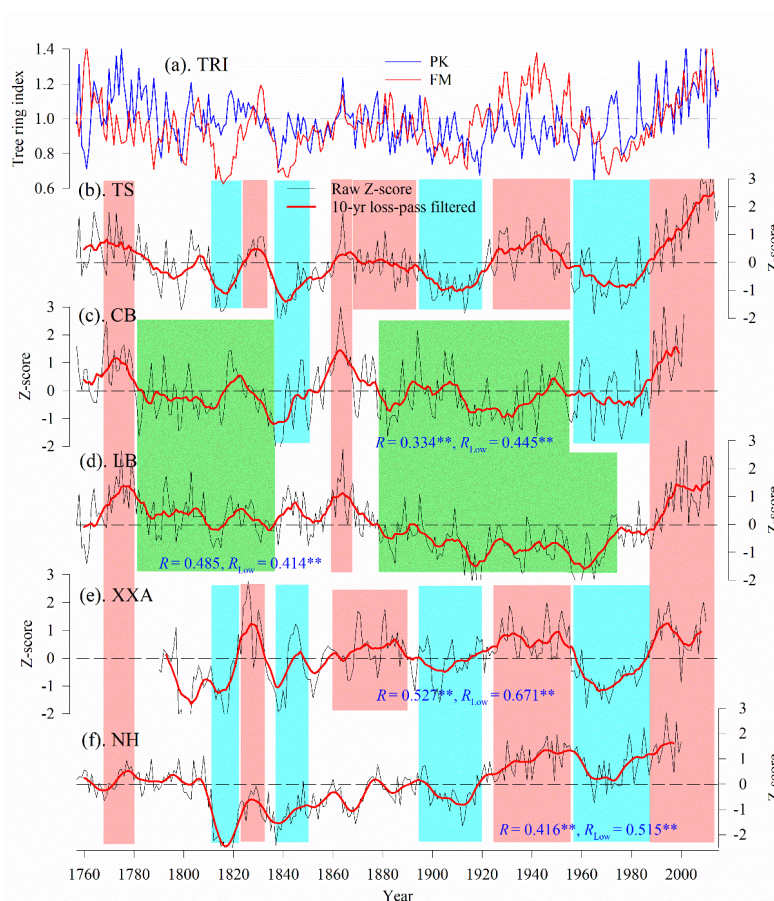
211 minimum temperatures are often accompanied by a long growing-season and a high photosynthetic efficiency, which results in wider
212 rings (Fritts, 1976). In contrast, trees tend to form narrow rings in years with low growing-season minimum temperatures.
213 As previous studies have shown, *P. koraiensis* and *F. mandshurica* show contrasting response patterns to rapid warming (Cao et al.,
214 2018;Zhu et al., 2015b;Zhu et al., 2020b;Wang et al., 2016). In the case of *P. koraiensis*, temperature sensitivity is slightly weakened
215 after warming (Zhu et al., 2015b). This divergence phenomenon has been reported by many studies, especially in northern forests
216 (D'Arrigo et al., 2008;Zhu et al., 2018a). Although many previous tree-ring studies from the surrounding area have suggested that this
217 divergence phenomenon is associated with temperature-induced drought stress (Zhu et al., 2018a;Zhu et al., 2015b), the exact causes
218 are still unknown. Other possible causes include nonlinear thresholds or time-dependent responses to rapid warming, the delayed
219 snowmelt and related changes in seasonality, the differential growth-climate relationships inferred for mean, maximum, and
220 minimum temperatures, and global dimming (D'Arrigo et al., 2008).
221 Unlike *P. koraiensis*, the growth of *F. mandshurica* has been significantly enhanced by warming, a result that is consistent those of
222 other studies of *F. mandshurica* in northeastern China (Cao et al., 2018;Zhu et al., 2020b). The reasons for this enhancement are still
223 not clear. Zhang et al. (2016) pointed out that the radial growth of *Larix gmelinii* is more sensitive to temperature after rapid warming
224 because of changes in the moisture availability caused by the permafrost thaw. Previous studies have shown that drought stress in
225 early spring is a key factor limiting vessel formation and tree growth (Zhu et al., 2020b). The enhanced temperature sensitivity of *F.*
226 *mandshurica* is likely related to the temporal coincidence between cambial activity and snowmelt and related changes in seasonality.
227 The unstable sensitivity of *P. koraiensis* or *F. mandshurica* to temperature (Fig. 3) has been proved widespread in northeast China
228 (Cao et al., 2018;Zhu et al., 2015b;Zhu et al., 2020b;Wang et al., 2016). Hence, previous temperature reconstructions based only on
229 tree-ring widths of *P. koraiensis* (Zhu et al., 2009;Shao and Wu, 1997;Lyu et al., 2016) or *F. mandshurica* (Zhang et al., 2007;Wang
230 et al., 2012;Yu, 2019) may have some uncertainty. Our results confirmed that the unstable sensitivity of *P. koraiensis* or *F.*
231 *mandshurica* to temperature before and after warming hindered the possibility of paleoclimate reconstruction based on single species
232 tree-ring data. Both two reconstruction models based on the combined *P. koraiensis* and combined *F. mandshurica* chronologies do
233 not pass the model test (Table 2). However, the opposite patterns in temperature sensitivity of *P. koraiensis* and *F. mandshurica* make
234 it possible to improve the performance of tree-ring-based temperature reconstruction by multiple tree species (Table 2).

235 4.2 Higher quality of our reconstruction and its comparison with regional records

236 In general, our reconstruction reflects warm/cold patterns that have been observed in other temperature records (Fig. 6) and local
237 historical documents (Wen, 2008) from northeastern China. This suggests that similar processes control temperatures across northeast



238 China. Spatial field correlations between our reconstructed temperature and the gridded $0.5^\circ \times 0.5^\circ$ growing-season temperatures are
239 significant ($p < 0.05$) across much of northeast Asia (Fig. S3). Compared with the existing reconstructed temperatures for the Changbai
240 Mountains, our reconstruction is more consistent with reconstructed temperatures from the nearby Xiaoxing'an Mountains of northeast
241 China (XXA, Zhu et al. (2015a)) and from the extratropical Northern Hemisphere (NH, Wilson et al. (2007)) at low- and high-
242 frequency scales (Fig. 6e-f). Common cold/warm periods and similar fluctuation patterns during the past two centuries indicate that
243 our reconstruction is accurate and reliable.



244
245 **Figure 6.** Comparison of temperature records in northeastern China and the extratropical Northern Hemisphere. (a) The tree-ring index
246 (TRI) of combined *P. koraiensis* (PK) and combined *F. mandshurica* (FM) in the northern Changbai Mountains. (b) The April-September
247 minimum temperature reconstruction in the northern Changbai Mountains in this study (TS). (c) The February-April mean temperature
248 reconstruction for the Changbai (CB) Mountains by Zhu et al., (2009). (d) The April-July minimum temperature reconstruction for the
249 Laobai (LB) Mountains by Lyu et al., (2017). (e) The February-March minimum temperature reconstruction for the Xiaoxing'an (XXA)
250 Mountains by Zhu et al., (2015). (e) The extratropical Northern Hemisphere (NH) temperature reconstruction by Wilson et al., (2007). All of
251 the above series were standardized using Z-scores; low-pass filtration was then carried out using a 10-year loess filter. Blue (cold) and red
252 (warm) shading indicate periods with good temperature consistency across reconstructions. The periods that are inconsistent with our



253 reconstruction are highlighted in green.

254 A significant positive correlation was found between our reconstruction and the February-April mean temperature (CB, Zhu et al.
255 (2009)) and April-July minimum temperature (LB, Lyu et al. (2016)) in the Changbai Mountains at low and high frequencies (Fig. 6c-
256 d). Although the three records display highly synchronous variations, there are several notable differences. The most obvious
257 differences occur in the years of 1800-1850 and 1870-1950, especially at low frequencies (Fig. 6a-d). These differences may be due to
258 the reconstruction bias of using a single species. The two temperature records (CB and LB in Fig. 6) in Changbai Mountains were both
259 based on tree-ring widths of *P. koraiensis* (Zhu et al., 2009;Lyu et al., 2016), which is known to have an unstable growth-climate
260 relationship (Zhu et al., 2015b). There are two temperature records based on the ring widths of *F. mandshurica* for the Changbai
261 Mountains (Yu, 2019;Wang et al., 2012), but we were unable to access these records. Nevertheless, a visual comparison of our
262 reconstruction and the two temperature sequences indicates some differences (Yu, 2019;Wang et al., 2012).

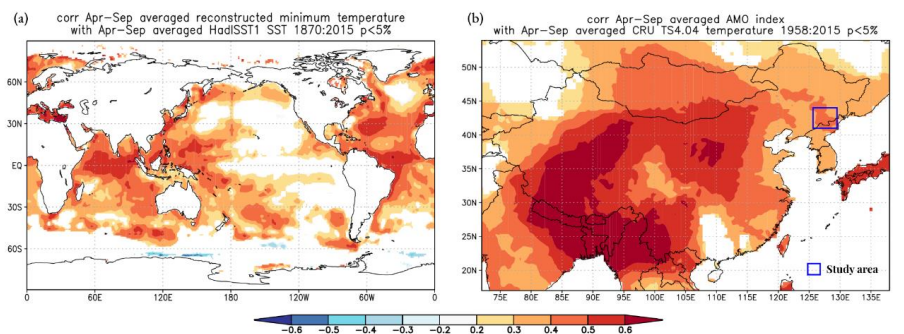
263 In general, our mixed-species temperature reconstruction shows absolute advantages, with higher accuracy and reliability than previous
264 temperature reconstructions that use only one species (*P. koraiensis* or *F. mandshurica*). This ingenious tree species mixing method
265 significantly improves the model stability and reliability. It provides a valuable reference for tree-ring-based paleoclimate
266 reconstructions in areas with unstable growth-climate relationships.

267 **4.3 Linkages to the Atlantic Multidecadal Oscillation**

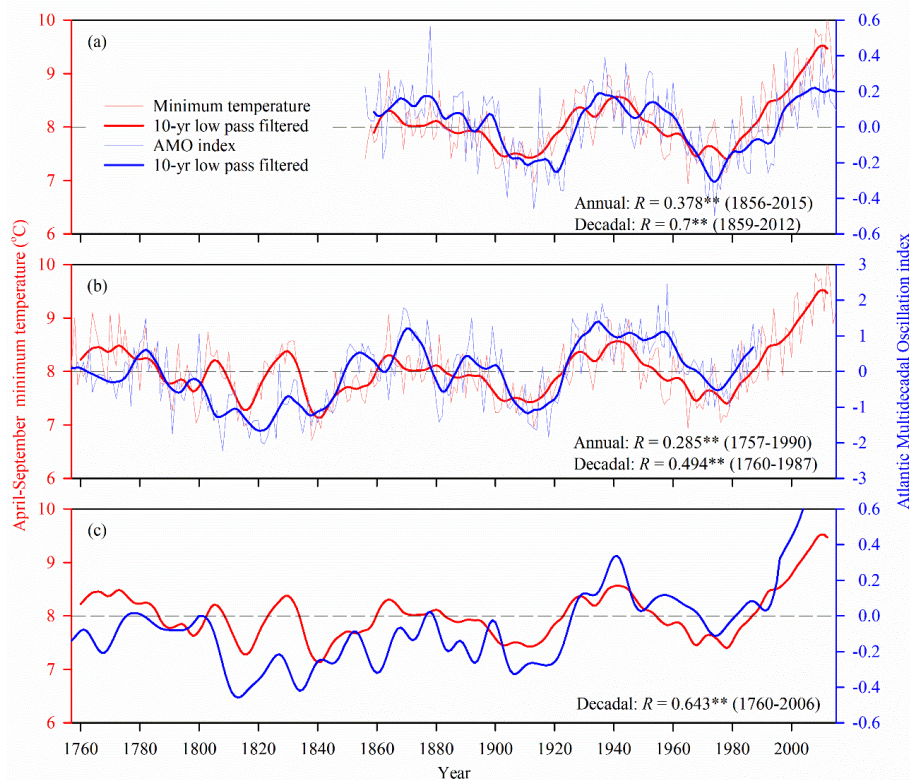
268 The Atlantic Multidecadal Oscillation (AMO) has been shown to play a key role in influencing global climate (Knight et al., 2006),
269 especially in North America (Nigam et al., 2011;Oglesby et al., 2012;Gan et al., 2019) and Europe (Vicente-Serrano and López-
270 Moreno, 2008;Brgel et al., 2020). In this study, we found that the AMO has a strong effect on the growing-season minimum
271 temperature in the northern Changbai Mountains, which is in line with previous tree-ring-based temperature reconstructions in
272 northeastern China (Zhu et al., 2015a;Zhu et al., 2017;Li and Wang, 2013;Lyu et al., 2016). Temperature in the northern Changbai
273 Mountains fluctuates on 59.6- and 78.4-year cycles, which is consistent with the 60-80-year cycle (AMO) of the North Atlantic SST
274 anomalies (Gray, 2004) (Fig. 7). We found strong and significant spatial correlations between our reconstructed temperature and the
275 SST anomalies over the Atlantic Ocean (Fig. 7a), and between the actual AMO index and the April-September land surface CRU
276 TS4.04 minimum temperature in the Changbai Mountains (Fig. 7b). These correlations reveal a potential linkage between the AMO
277 and the temperature in the northern Changbai Mountains. Similar significant ($p<0.01$) and positive correlations exist between the
278 temperature reconstruction for the northern Changbai Mountains and the actual (annual: $R=0.378$, decadal: $R=0.7$) (Enfield et al.,
279 2001) and reconstructed (Gray: annual: $R=0.285$, decadal: $R=0.494$; Mann: decadal: $R=0.643$) (Mann et al., 2009;Gray, 2004) AMO



280 indices at both annual and decadal scales (Fig. 8), further confirming the effect of the AMO on temperature in the Changbai
281 Mountains.



282
283 **Figure 7.** The influence of the AMO on the growing-season minimum temperature in the northern Changbai Mountains. (a) Spatial
284 correlation between reconstructed April-September averaged minimum temperatures with Sea Surface Temperatures at a global scale. The
285 spatial correlation was calculated for April-September and covers the period from 1870 to 2015. (b) Spatial correlation of the actual AMO
286 (Enfield et al., 2001) with April-September land surface minimum temperature from the CRU TS4.04 for the period 1958-2015. Maps with
287 filled p-values > 5% were masked out.

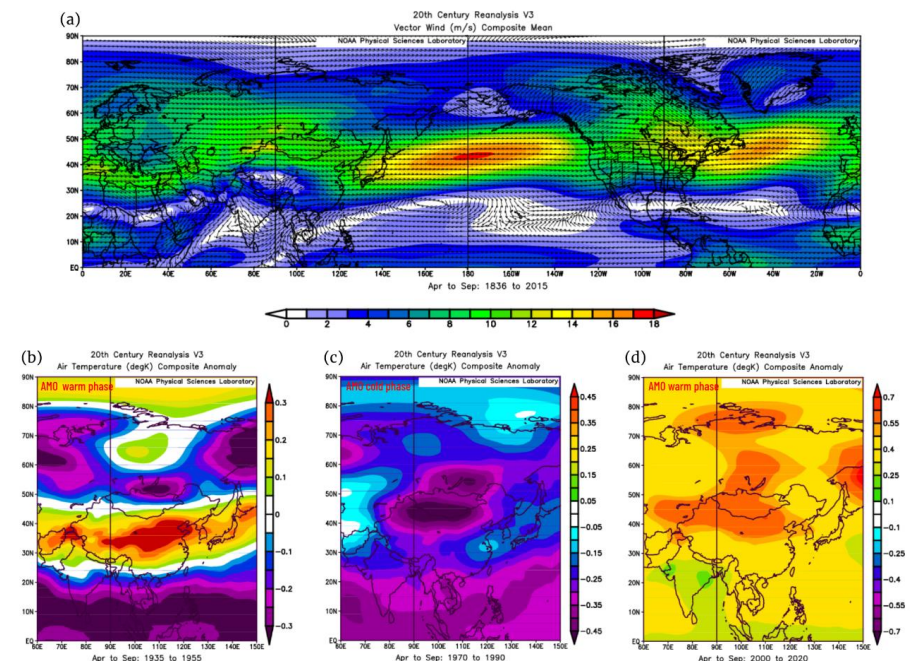


288
289 **Figure 8.** The influence of the Atlantic Multidecadal Oscillation (AMO) on the growing-season minimum temperature in the northern
290 Changbai Mountains. (a) The reconstructed temperature and the actual AMO index from Enfield et al., (2001). (b) The reconstructed



291 temperature and the reconstructed annual Sea Surface Temperature anomalies for the North Atlantic (AMO index) from Gray (2001). (c)
292 The reconstructed temperature and the reconstructed AMO index from Mann et al., (2009). The red line in (a)-(c) denotes the reconstructed
293 growing-season minimum temperature from this study (thin line) and its 10-year low-pass loess filter (bold line). The blue line in (a)-(c)
294 denotes the AMO index from this study (thin line) and its 10-year low-pass loess filter (bold line). Correlations are shown in each panel.
295 Double asterisks denote correlation significance at the 99% confidence level.

296 Previous studies have also confirmed that the AMO can strongly influence China's climate (Li et al., 2015; Wang et al., 2013), with
297 impacts on temperature and drought in the southwest (Fang et al., 2019; Shi et al., 2017; Zeng et al., 2019), northwest (Chen et al.,
298 2013), and northeast (Liu et al., 2019; Zhu et al., 2018b; Zhu et al., 2020a). The SST anomalies in the North Atlantic or AMO can
299 change oceanic-atmospheric-land surface interactions and directly affect the local climate in eastern Asia (Wang et al., 2013; Wang et
300 al., 2009). Temperature in the northern Changbai Mountains is significantly ($p < 0.01$) positively correlated with the actual AMO
301 indices from prior April to current September (Table S3). The composite April-September air temperature anomaly for the three
302 AMO extreme periods during the past 100 years also confirms our results (Fig. 9). Temperature over our study area had a positive
303 temperature anomaly during the two warm periods from 1935 to 1955 and 2000 to 2020. However, it has a negative anomaly during
304 the cold periods from 1970 to 1990 (Fig. 9b-d). The 500-mb vector wind data confirm that a strong atmospheric circulation
305 originating in the North Atlantic traverses all of Eurasia before dropping over northeast Asia (Fig. 9a). This circulation brings
306 warm/cold air masses from the Atlantic Ocean and Eurasia to northeastern China (Fig. 9a). The AMO may also affect temperature in
307 the Changbai Mountains by modulating other large-scale circulation patterns. For example, large-scale circulation related to Pacific
308 Ocean-atmospheric coupling processes, such as the El Niño-Southern Oscillation and the Pacific Decadal Oscillation, could affect
309 local temperatures in northeastern China (Zhang and Thomas, 2007; Dong et al., 2006; Zhu et al., 2017).



310

311 **Figure 9.** The (a) averaged April to September 500-mb vector wind in the Northern Hemisphere and the (b-d) 20th century reanalysis V3 air
312 temperature composite anomaly for three different AMO phase periods during the growing-season (April-September). (b) Warm phase
313 from 1935 to 1955, (c) cold phase from 1970 to 1990, and (d) warm phase from 2000 to 2020.

314 5 Conclusion

315 We propose a novel tree-species mixing method to improve the accuracy of tree-ring-based reconstructions in areas with unstable
316 growth-climate relationships. This method significantly improves the model stability and reliability of a temperature
317 reconstruction for the northern Changbai Mountains. During the calibration period from 1958 to 2015, the model explains 68%
318 of the growing-season minimum temperature variation. During the past 259 years (AD 1757-2015), five warm periods (1762-
319 1776, 1828-1831, 1927-1930, 1936-1947, and 1991-2012) and five cold periods occurred (1797-1800, 1811-1820, 1836-1856,
320 1898-1918 and 1956-1982). Our reconstruction shows good consistency and high accuracy with nearby tree-ring-based
321 reconstructions and historical records. This reconstruction successfully captures the warming observed in the instrumental record
322 since the 1980s. Within the 259-year record, we find significant ($p < 0.01$) annual cycle peaks at 2.7, 3, and 3.5 years, and decadal
323 cycle peaks at 59.6 and 78.4 years. The AMO plays a key role in modulating temperature in the northern Changbai Mountains.
324

325 **Data availability.** The temperature reconstruction in the Changbai Mountains will be uploaded to NOAA, and all the data published in
326 this study will be available for non-commercial scientific purposes.

327 **Author contributions.** For this article, LZ and XW conceived the study; LZ, HZ, DY and XZ collected the data; LZ, DC, DY, YZ,
328 HL and XW elaborated the methodology; LZ, SL, ZL, YZ and DY analysed the data; LZ, SL and XW led the writing of the manuscript;
329 LZ, DC, WS, ZL, YZ and XW revised the manuscript.

330 **Competing interests.** The authors declare that they have no conflict of interest.



331 **Acknowledgments.** This research was supported by the Science and Technology Innovation Program of Hunan Province (2020RC2058), the
332 China Postdoctoral Science Foundation (2020M682600), the Research Foundation of the Bureau of Education in Hunan Province
333 (20B627), and the Start-up Scientific Research Foundation for the Introduction of Talents at the Central South University of Forestry
334 and Technology (2020YJ012).

335 **References**

- 336 Allen, C. D., Macalady, A. K., Chenchouni, H., Bachelet, D., McDowell, N., Vennetier, M., Kitzberger, T., Rigling, A., Breshears, D.
337 D., Hogg, E. H., Gonzalez, P., Fensham, R., Zhang, Z., Castro, J., Demidova, N., Lim, J. H., Allard, G., Running, S. W., Semerci, A.,
338 and Cobb, N.: A global overview of drought and heat-induced tree mortality reveals emerging climate change risks for forests, *Forest*
339 *Ecol Manag*, 259, 660-684, 10.1016/j.foreco.2009.09.001, 2010.
- 340 Anchukaitis, K. J., Wilson, R., Briffa, K. R., Buntgen, U., Cook, E. R., D'Arrigo, R., Davi, N., Esper, J., Frank, D., Gunnarson, B. E.,
341 Hegerl, G., Helama, S., Klesse, S., Krusic, P. J., Linderholm, H. W., Myglan, V., Osborn, T. J., Zhang, P., Rydval, M., Schneider, L.,
342 Schurer, A., Wiles, G., and Zorita, E.: Last millennium Northern Hemisphere summer temperatures from tree rings: Part II, spatially
343 resolved reconstructions, *Quaternary Sci Rev*, 163, 1-22, 10.1016/j.quascirev.2017.02.020, 2017.
- 344 Brgel, F., Frauen, C., Neumann, T., and Meier, H. E. M.: The Atlantic Multidecadal Oscillation controls the impact of the North
345 Atlantic Oscillation on North European climate, *Environ Res Lett*, 15, 104025, 2020.
- 346 Bunn, A. G.: A dendrochronology program library in R (dplR), *Dendrochronologia*, 26, 115-124,
347 <https://doi.org/10.1016/j.dendro.2008.01.002>, 2008.
- 348 Cao, J., Zhao, B., Gao, L., Li, J., Li, Z., and Zhao, X.: Increasing temperature sensitivity caused by climate warming, evidence from
349 Northeastern China, *Dendrochronologia*, 51, 101-111, 2018.
- 350 Chen, F., Yuan, Y., Chen, F., Wei, W., Yu, S., Chen, X., Fan, Z., Zhang, R., Zhang, T., and Shang, H.: A 426-year drought history for
351 Western Tian Shan, Central Asia, inferred from tree rings and linkages to the North Atlantic and Indo-West Pacific Oceans, *The*
352 *Holocene*, 23, 1095-1104, 2013.
- 353 D'Arrigo, R., Wilson, R., Liepert, B., and Cherubini, P.: On the 'Divergence Problem' in Northern Forests: A review of the tree-ring
354 evidence and possible causes, *Glob Planet Change*, 60, 289-305, 2008.
- 355 Dong, B. W., Sutton, R. T., and Scaife, A. A.: Multidecadal modulation of El Nino-Southern Oscillation (ENSO) variance by Atlantic
356 Ocean Sea Surface Temperatures, *Geophys Res Lett*, 33, 93-93, 2006.
- 357 Enfield, D. B., Mestas - Nuez, A. M., and Trimble, P. J.: The Atlantic Multidecadal Oscillation and its relation to rainfall and river
358 flows in the continental U.S, *Geophys Res Lett*, 28, 2077-2080, 2001.
- 359 Fang, K., Guo, Z., Chen, D., Wang, L., Dong, Z., Zhou, F., Zhao, Y., Li, J., Li, Y., and Cao, X.: Interdecadal modulation of the
360 Atlantic Multi-decadal Oscillation (AMO) on southwest China's temperature over the past 250 years, *Clim Dynam*, 52, 2055-2065,
361 2019.
- 362 Fritts, H. C.: *Tree Rings and Climate*, edited by: Fritts, H. C., Academic Press, London, 1-567 pp., 1976.
- 363 Gan, Z., Guan, X., Kong, X., Guo, R., Huang, H., Huang, W., and Xu, Y.: The Key Role of Atlantic Multidecadal Oscillation in
364 Minimum Temperature over North America during Global Warming Slowdown, *Earth Space Sci*, 6, 387-398, 2019.
- 365 Gray, S. T.: A tree - ring based reconstruction of the Atlantic Multidecadal Oscillation since 1567 A.D, *Geophys Res Lett*, 31, 261-
366 268, 2004.
- 367 Holmes, R. L.: Computer-assisted quality control in tree-ring dating and measurement, *Tree-Ring Bulletin*, 43, 69-78, 1983.
- 368 IPCC: *Global Warming of 1.5°C*, Intergovernmental Panel on Climate Change, Geneva, Switzerland, 2018.
- 369 Knight, J. R., Folland, C. K., and Scaife, A. A.: Climate impacts of the Atlantic Multidecadal Oscillation, *Geophys Res Lett*, 33,



- 370 2006.
- 371 Li, M., and Wang, X. C.: Climate-growth relationships of three hardwood species and Korean pine and minimum temperature
372 reconstruction in growing season in Dunhua, China, *J Nanjing Forestry Uni (Natural Sciences Edition)*, 3, 29-34, 2013.
- 373 Li, S., Jing, Y., and Luo, F.: The potential connection between China surface air temperature and the Atlantic Multidecadal
374 Oscillation(AMO) in the Pre-industrial Period, *Sci China Earth Sci*, 10, 1814-1826, 2015.
- 375 Liu, H., Park Williams, A., Allen, C. D., Guo, D., Wu, X., Anenkhonov, O. A., Liang, E., Sandanov, D. V., Yin, Y., Qi, Z., and
376 Badmaeva, N. K.: Rapid warming accelerates tree growth decline in semi-arid forests of Inner Asia, *Global Change Biol*, 19, 2500-
377 2510, 10.1111/gcb.12217, 2013.
- 378 Liu, R., Liu, Y., Li, Q., Song, H., Li, X., Sun, C., Cai, Q., and Song, Y.: Seasonal Palmer drought severity index reconstruction using
379 tree-ring widths from multiple sites over the central-western Da Hinggan Mountains, China since 1825 AD, *Clim Dynam*, 1-14,
380 <https://doi.org/10.1007/s00382-019-04733-0>, 2019.
- 381 Lyu, S., Li, Z., Zhang, Y., and Wang, X.: A 414-year tree-ring-based April–July minimum temperature reconstruction and its
382 implications for the extreme climate events, northeast China, *Clim Past*, 12, 1879-1888, 2016.
- 383 Mann, M. E., and Lees, J. M.: Robust estimation of background noise and signal detection in climatic time series, *Climatic Change*,
384 33, 409-445, 1996.
- 385 Mann, M. E., Zhang, Z. H., Rutherford, S., Bradley, R. S., Hughes, M. K., Shindell, D., Ammann, C., Faluvegi, G., and Ni, F. B.:
386 Global Signatures and Dynamical Origins of the Little Ice Age and Medieval Climate Anomaly, *Science*, 326, 1256-1260,
387 10.1126/science.1177303, 2009.
- 388 Nigam, S., Guan, B., and Ruiz-Barradas, A.: Key role of the Atlantic Multidecadal Oscillation in 20th century drought and wet
389 periods over the Great Plains, *Geophys Res Lett*, 38, 239-255, 2011.
- 390 Oglesby, R., Feng, S., Hu, Q., and Rowe, C.: The role of the Atlantic Multidecadal Oscillation on medieval drought in North
391 America: Synthesizing results from proxy data and climate models, *Global Planet Change*, 84-85, 56-65, 2012.
- 392 Shao, X. M., and Wu, X. D.: Reconstruction of climate change on Changbai Mountain, Northeast China using tree-ring data,
393 *Quaternary Sci*, 17, 76-85, 1997.
- 394 Shi, S., Li, J., Shi, J., Zhao, Y., and Huang, G.: Three centuries of winter temperature change on the southeastern Tibetan Plateau and
395 its relationship with the Atlantic Multidecadal Oscillation, *Clim Dynam*, 49, 2017.
- 396 Stokes, M. A., and Smiley, T. L.: An introduction to tree-ring dating, University of Chicago Press, Chicago., xiv, 73 p. pp., 1968.
- 397 Vicente-Serrano, S. M., and López-Moreno, J. I.: Nonstationary influence of the North Atlantic Oscillation on European
398 precipitation, *J Geophys Res-Atmos*, 113, D20120, doi: 10.1029/2008JD010382, 2008.
- 399 Wang, J., Yang, B., Ljungqvist, F. C., and Zhao, Y.: The relationship between the Atlantic Multidecadal Oscillation and temperature
400 variability in China during the last millennium, *J Quaternary Sci*, 28, 653-658, 2013.
- 401 Wang, W., Zhang, J., Dai, G., Wang, X., Han, S., Zhang, H., and Wang, Y.: Variation of autumn temperature over the past 240 years
402 in Changbai Mountains of Northeast China: A reconstruction with tree-ring records, *Chinese J Ecol*, 31, 787-793, 2012.
- 403 Wang, X., Zhang, M., Ji, Y., Li, Z., and Zhang, Y.: Temperature signals in tree-ring width and divergent growth of Korean pine
404 response to recent climate warming in northeast Asia, *Trees-Struct Funct*, 31, 1-13, 2016.
- 405 Wang, Y., Li, S., and Luo, D.: Seasonal response of Asian monsoonal climate to the Atlantic Multidecadal Oscillation, *J Geophys*
406 *Res-Atmos*, 114, D02112, 10.1029/2008JD010929, 2009.
- 407 Wen, k.: Meteorological disasters dictionary of China, edited by: Qin, Y., Meteorological Press, 2008.
- 408 Wigley, T. M. L., Briffa, K. R., and Jones, P. D.: On the Average Value of Correlated Time Series, with Applications in
409 Dendroclimatology and Hydrometeorology, *J Climate Appl Meteor*, 23, 201-213, 1984.
- 410 Wilson, R., D'Arrigo, R., Buckley, B., Büntgen, U., Esper, J., Frank, D., Luckman, B., Payette, S., Vose, R., and Youngblut, D.: A



- 411 matter of divergence: Tracking recent warming at hemispheric scales using tree ring data, *J Geophys Res*, 112,
412 <https://doi.org/10.1029/2006JD008318>, 2007.
- 413 Wilson, R., Anchukaitis, K., Briffa, K. R., Buntgen, U., Cook, E., D'Arrigo, R., Davi, N., Esper, J., Frank, D., Gunnarson, B., Hegerl,
414 G., Helama, S., Klesse, S., Krusic, P. J., Linderholm, H. W., Myglan, V., Osborn, T. J., Rydval, M., Schneider, L., Schurer, A., Wiles,
415 G., Zhang, P., and Zorita, E.: Last millennium northern hemisphere summer temperatures from tree rings: Part I: The long term
416 context, *Quaternary Sci Rev*, 134, 1-18, [10.1016/j.quascirev.2015.12.005](https://doi.org/10.1016/j.quascirev.2015.12.005), 2016.
- 417 Yu, J.: Response of radial growth of main tree species of broad-leaved Korean pine forest to climate change in Changbai Mountain
418 and temperature reconstruction, 1-111, Beijing Forestry University, Beijing, 2019.
- 419 Zeng, A. Y., Zhou, F., Li, W., Bai, Y., and Zeng, C.: Tree-ring indicators of winter-spring temperature in Central China over the past
420 200 years, *Dendrochronologia*, 58, 125634, 2019.
- 421 Zhang, H., Han, S., Li, Y., and Zhang, J.: Reconstruction of temporal variations of precipitation in Changbai Mountains area over
422 past 240 years by using tree-ring width data, *Chinese J Ecol*, 26, 1924-1929, 2007.
- 423 Zhang, R., and Thomas, D. L.: Impact of the Atlantic Multidecadal Oscillation on North Pacific climate variability, *Geophys Res*
424 *Lett*, 34, 229-241, 2007.
- 425 Zhang, X. L., Bai, X. P., Chang, Y. X., and Chen, Z. J.: Increased sensitivity of Dahurian larch radial growth to summer temperature
426 with the rapid warming in Northeast China, *Trees-Struct Funct*, 30, 1799-1806, [10.1007/s00468-016-1413-6](https://doi.org/10.1007/s00468-016-1413-6), 2016.
- 427 Zhu, H. F., Fang, X. Q., Shao, X. M., and Yin, Z.: Tree ring-based February-April temperature reconstruction for Changbai Mountain
428 in Northeast China and its implication for East Asian winter monsoon, *Clim Past*, 5, 661-666, 2009.
- 429 Zhu, L., Li, Z., Zhang, Y., and Wang, X.: A 211 - year growing season temperature reconstruction using tree - ring width in
430 Zhangguangcai Mountains, Northeast China: linkages to the Pacific and Atlantic Oceans, *Int J Climatol*, 37, 2017.
- 431 Zhu, L., Cooper, D. J., Yang, J., Zhang, X., and Wang, X.: Rapid warming induces the contrasting growth of Yezo spruce (*Picea*
432 *jezoensis* var. *microsperma*) at two elevation gradient sites of northeast China, *Dendrochronologia*, 50, 52-63, 2018a.
- 433 Zhu, L., Yao, Q., Cooper, D. J., Han, S., and Wang, X.: Response of *Pinus sylvestris* var. *mongolica* to water change and drought
434 history reconstruction in the past 260 years, northeast China, *Clim Past*, 14, 1213-1228, 2018b.
- 435 Zhu, L., Cooper, D. J., Han, S., Yang, J., Zhang, Y., Li, Z., Zhao, H., and Wang, X.: Influence of the Atlantic Multidecadal Oscillation
436 on drought in northern Daxing'an Mountains, Northeast China, *CATENA*, 105017, <https://doi.org/10.1016/j.catena.2020.105017>,
437 2020a.
- 438 Zhu, L., Cooper, D. J., Yuan, D., Li, Z., Zhang, Y., Liang, H., and Wang, X.: Regional scale temperature rather than precipitation
439 determines vessel features in earlywood of Manchurian ash in temperate forests, *J Geophys Res-Bioge*, 125, JGRG21771,
440 [10.1029/2020JG005955](https://doi.org/10.1029/2020JG005955), 2020b.
- 441 Zhu, L. J., Li, S. Y., and Wang, X. C.: Tree-ring Reconstruction of Feb-Mar Mean Minimum Temperature Back to AD 1790 in
442 Yichun, Northeast China, *Quaternary Sci*, 35, 1175-1184, [10.11928/j.issn.1001-7410.2015.05.](https://doi.org/10.11928/j.issn.1001-7410.2015.05.), 2015a.
- 443 Zhu, L. J., Yang, J. W., Zhu, C., and Wang, X. C.: Influences of gap disturbance and warming on radial growth of *Pinus koraiensis*
444 and *Abies nephrolepis* in Xiaoxing'an Mountain, Northeast China, *Chinese J Ecol*, 34, 2085-2095, 2015b.